THICKNESS OF PYROCLASTIC DEPOSITS FOR AESTUUM REGION: INITIAL RESULTS FROM KAGUYA LUNAR RADAR SOUNDER. Yuanzheng Xiao[1], Wenzhe Fa[1], and Takao Kobayashi[2], [1]Institute of Remote Sensing and Geographical Information System, Peking University, Beijing 100871, China (yzxiao@pku.edu.cn; wzfa@pku.edu.cn). [2] Earth Planetary Science Department, Korea Institute of Geoscience and Mineral Resources, Daejeon 305-350, Korea.

Introduction: Both Earth-based and orbital remote sensing observations have found more than 100 lunar pyroclastic deposits (LPDs) that distributed widely across the lunar surface. These low albedo units are mostly observed in the highlands adjacent to maria or within floor-fractured craters, and they are thought to be formed from volcanic eruption during Imbrian/Eratosthenian periods [1]. Thicknesses of LPDs and their spatial distribution provides important clues for understanding the styles and scales of volcanic eruptions and also the emplacement of lava flows.

Surfaces of most pyroclastic deposits are usually very smooth, and dielectric loss of its fine-grained dark materials is relative low. A radar wave at proper frequency can penetrate tens to hundreds of meters below lunar surface, and therefore can disclose information about lunar subsurface stratification. Radar instruments in recent lunar missions, such as Kaguya Lunar Radar Sounder (LRS) and Miniature Radio Frequency (Mini-RF) onboard Lunar Reconnaissance Orbiter (LRO), provide an opportunity for quantitative study of subsurface structure of LPDs.

In this study, the Kaguya LRS data are used to investigate subsurface layering structure for Aestuum region. We found that most pyroclastic deposits have distinct subsurface echoes, though for some regions subsurface echoes are very difficult to be identified because of surface clutters. To identify subsurface echoes, high resolution lunar surface digital elevation model is used to simulate lunar surface clutters. Then a two-layer model is used to estimate the thicknesses of pyroclastic deposits and dielectric constant of underlying layer. Our results show that thickness for most areas in Aestuum region varies from 100 m to 300 m, and the maximum thickness can reach to more than 400 m.

LRS Images for Pyroclastic Deposits: Kaguya LRS transmitted a frequency modulated continuous wave at 5 MHz with a bandwidth of 2 MHz. The nominal penetration depth is about 500 m for a typical pyroclastic deposits with a dielectric constant of 2.6+0.03i. The range resolution is about 75 m in vacuum and the pulse repetition frequency (PRF) is 20 Hz [2][3]. LRS has observed more than 90% of lunar surface that covers most pyroclastic deposits.

In this study, pyroclastic deposits region Aestuum (Lat. 6.6°N, Lon. 5.9°W; Area 10357 km^2) are analyzed using LRS data. Figure 1 shows the tracks of LRS data for Aestuum region in the Lunar Reconnaissance Orbiter Camera (LROC) Wide Angle Camera (WAC) image. The dark regions within the blue curves are our identified pyroclastic deposits that based on the rules by Gaddis et al. [1]. The vertical lines in Figure 1 represent LRS tracks, and each contains about 1900 independent observations.

Figure 2a shows LRS image that along the green line in Figure 1, where the abscissa represents the surface latitude for subradar points and the ordinate indicates the relative range of radar echoes with a range offset of 96.5 km (the altitude of the spacecraft is about 96 km). It can be seen that surface nadir echo is very strong for all regions. There are two distinct echoes for regions with latitude between 4.5°N to 6.0°N. The second echo with range about 0.5 km is most probably from subsurface interface, because this peak cannot be found in the simulated surface clutters. Careful analysis shows that the regions with subsurface echoes correspond to the dark pyroclastic deposits regions along the green line in Figure 1.

To see it in more details, Figure 2b and 2c show the cross sections for the pyroclastic region and a normal surface, respectively. It can be seen that subsurface echoes are very clear for pyroclastic regions whereas there is almost no apparent subsurface echo for a normal surface. Analyses of LRS images for other tracks of this region show that most parts have clear subsurface echoes.

As an example, Figure 3 shows the variation of LRS echo strength as a function of apparent range for the location with latitude of 4.69°N and longitude of 9.01°W (the cyan point in Figure 1). It can be seen that surface nadir echo is much stronger than subsurface echoes, and the range between surface and subsurface echo is about 675 m. We also found several regions where surface echoes are smaller than subsurface echoes, which might be caused by different situations for the dielectric contrast between the pyroclastic deposits and subsurface layers.

Models and Results: A two-layer model is used to investigate subsurface structure of pyroclastic deposits, i.e., a pyroclastic deposits layer (Layer 1) atop the underlying bedrock (Layer 2). The dielectric constant of the pyroclastic deposits is ε_1 and that of underlying bedrock is ε_2. Surface echo strength correlates with the Fresnel reflectivity, whereas subsurface echo strength can be modeled by considering the transmission, attenuation and reflection of radar wave through the pyroclastic deposits layer. Then, the ratio of intensity between surface and subsurface echo can be expressed as

$$\frac{I_{01}}{I_{12}} = \frac{r_{01}}{\left(1-r_{01}\right)^2 r_{12} \exp\left(-\frac{4\pi}{\lambda}\frac{\varepsilon_1''}{\sqrt{\varepsilon_1'}}d\right)} \quad (1)$$

where I_{01} and I_{12} are intensities of surface and subsurface echoes, r_{ij} (i=0,1 and j=1,2) is the reflectivity between layer i and j, and d is the thickness of pyroclastic layer.

From the apparent range of the received echoes, thickness of pyroclastic deposits can be estimated as

$$d = \frac{R_{sub} - R_{sur}}{\sqrt{\varepsilon_1'}} \quad (2)$$

where R_{sur} and R_{sub} are surface and subsurface range. In addition, as the ratio of intensity between surface and subsurface echo is obtained, real part of the dielectric constant for the underlying layer can be obtained numerically from equation (1).

Based on Clementine UVVIS data [4] and the relation between dielectric constant and composition, dielectric constant of the pyroclastic is estimated as 2.56+ 0.037i for this region [5]. From Figure 3, the range difference between subsurface to surface echo is 675 m, and then thickness of the pyroclastic deposits is estimated to be 421 m. The ratio of surface echo to subsurface echo is 4.195, and then the real part of the dielectric constant of the underlying layer is estimated to be 5.5.

Using the same approach, the mean thickness for pyroclastic deposits in this region is estimated to be about 300 m, with a maximum value around 425 m (locates with Latitude of 5.11°N and Longitude of 8.70°W). We found thickness of pyroclastic deposits decreases with the increased distance from the center.

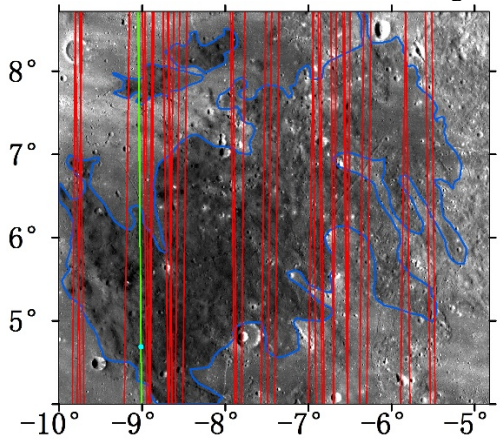

Figure 1: LRS tracks for Aestuum pyroclastic deposits. The blue curve indicates the margin of the pyroclastic deposits, and the vertical lines are the tracks of sub-satellite points for LRS data.

Conclusions: In this study, Kaguya LRS images are used to analyze subsurface properties for pyroclastic deposits at Aestuum region. It is clearly that subsurface echoes can be identified in LRS images and two or more layers can be distinguished. Our analyses based on a two-layer model show that thickness of pyroclastic deposits for Aestuum region is about 400 m as a maximum and most parts of Aestuum can reach to more than 100 meter. In addition, real part of dielectric constant of subsurface layer in the analyzed region is estimated to be 5.5. We are now doing a global study of the pyroclastic deposits thickness using the same dataset, and the details will be presented in the conference.

Acknowledgements: This work supported by the National Natural Science Foundation of China (No. 11203002).

References: [1] Gaddis L. R. et al. (2003) *Icarus*, *161*, 262-280. [2] Kobayashi T. et al. (2011) *IEEE Trans. Geosci. Remote Sens*., *50*, 2161–2174. [3] Ono T. et al. (2010) *Space Sci. Rev.*, 154, 145-192 [4] Lucey P. G. et al. (2000) *JGR*, *105 (E8*), 20,297-20,305. [5] Fa W. and Wieczorek M. A. (2012) *Icarus*, *218*, 771-787.

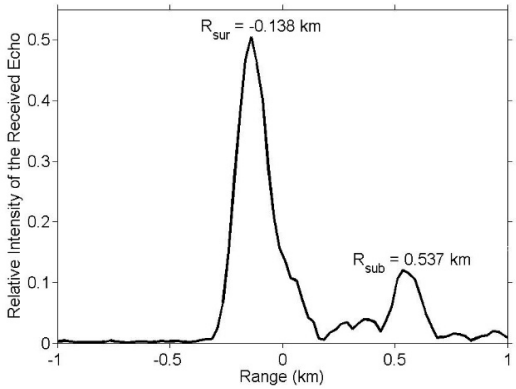

Figure 3: LRS echo intensity as a function of range for the location with Latitude of 4.69°N and Longitude of 9.01°W. The two echo peaks are from surface and subsurface, respectively.

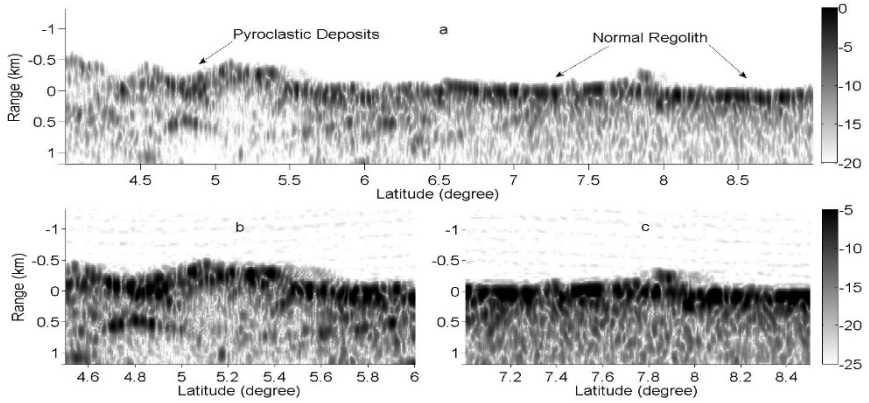

Figure 2: LRS image for the green line in Figure 1 with a range offset of 96.5 km. Cross section of LRS image for pyroclastic deposits (b) and for a normal regolith (c).